J. Fluid Mech. (1985), *vol.* 158, *pp.* 153–175
Printed in Great Britain

Wave-power absorption by an oscillating water column in a channel

By O. MALMO
Norwegian Hydrotechnical Laboratory, P.O. Box 4118-Valentinlyst, N-7001 Trondheim

AND A. REITAN
Department of Physics, College of Arts and Science, University of Trondheim, N-7055 Dragvoll

(Received 5 March 1984 and in revised form 16 January 1985)

Wave-power absorption by an oscillating water column in a channel is studied within linear theory, and for different boundary conditions regarding the regions between the absorber and the channel walls. Particular attention is given to the effect of placing projecting sidewalls in front of the column.

1. Introduction

The oscillating water column is one of several promising devices for absorption of energy from ocean waves. One of the earlier theoretical studies of oscillating water columns is that by Evans (1978), and other relevant calculations have been performed, e.g. by Falcão & Sarmento (1980) and Evans (1982*a*). We also mention the papers on resonant ducts by Lighthill (1979), Simon (1981) and Thomas (1981).

Later, the present authors and their collaborators (Ambli *et al.* 1982) presented the idea of improving the performance of an oscillating water column by the addition of two projecting sidewalls. For the sake of brevity, at the same time we coined the name 'harbour' for the area between these sidewalls, although its purpose is of course the opposite of that of an ordinary harbour. The effect of harbours in connection with this and other wave-power devices has subsequently also been studied by Evans (1982*b*) and Count & Evans (1984).

In the present paper our ideas concerning oscillating water columns with harbours are elaborated in more detail. For now we limit ourselves to the case of one absorber symmetrically placed in a channel, or, equivalently, an infinite row of identical and equidistant absorbers subjected to normally incident waves.

2. The absorbing system

We consider an idealized system for wave-power absorption as shown in figure 1. The pressure chamber has length a, width b and height H above the water surface, and is separated from a harbour of length l by an infinitely thin barrier of depth d. The harbour has the same width b as the chamber, and the system is placed symmetrically in a channel of width c. The water depth h is taken to be constant.

The regions at the sides and back of the absorber are either accessible to the channel waves or made inaccessible by a reflecting wall or an absorbing beach at the level of the harbour mouth.

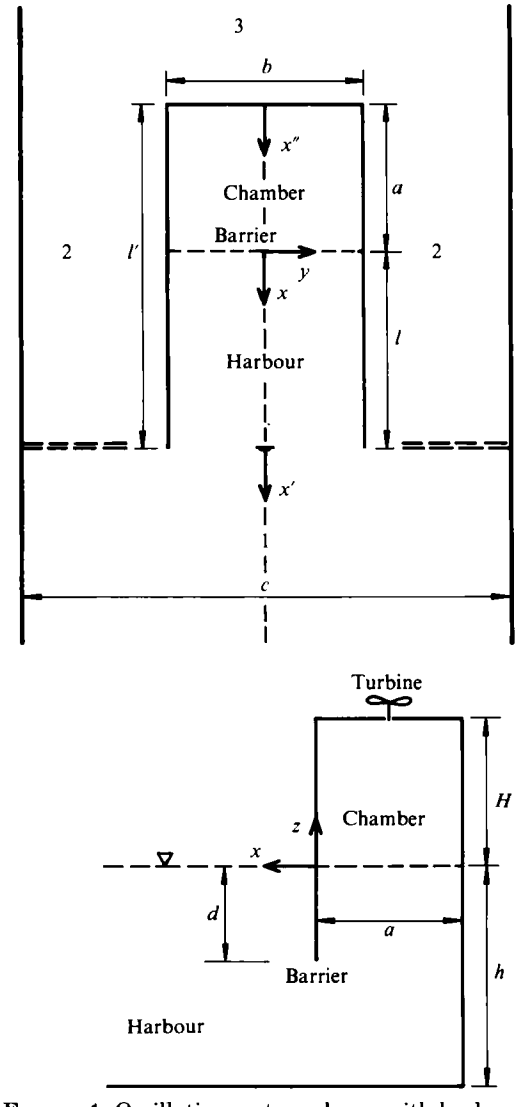

FIGURE 1. Oscillating water column with harbour.

The air turbine connected with the pressure chamber is assumed to be linear, i.e. the amplitude of the air flow is presumed proportional to the amplitude of the chamber pressure. The phases of these quantities need not, however, necessarily coincide.

3. Generalities

We are here concerned with harmonic wave motion at a given angular frequency ω, and described by a complex velocity potential $\hat{\phi}(x, y, z, t) = \phi(x, y, z) \exp(i\omega t)$. It has been shown by Evans (1982*a*) that in order to calculate the power absorbed by a system such as that in figure 1 within linear theory and for a given amplitude of the incoming wave we need just three pieces of information about the system:

(1) the volume flux through the surface of the chamber when the latter is open, i.e. without the roof and turbine, and the system is exposed to an incoming wave; (2) the admittance of the system, which is a measure of the volume flux through the chamber surface caused by an imposed harmonic chamber pressure; (3) the turbine constant, i.e. the volume flux of air through the turbine divided by the driving pressure.

We find it convenient to work with the mean wave amplitudes in the chamber rather than the corresponding volume fluxes. If an incoming wave with amplitude η_0 produces a wave $\hat{\eta}_C(x,y,t) = \eta_C(x,y)\exp(i\omega t)$ in the chamber we then define the ratio

$$\begin{aligned}\xi_C &= \langle \eta_C(x,y)\rangle/\eta_0 \\ &= (\eta_0 ab)^{-1}\int_{-a}^{0} dx \int_{-\frac{1}{2}b}^{\frac{1}{2}b} dy\, \eta_C(x,y),\end{aligned} \tag{3.1}$$

and use the notation ξ_0 for the value of ξ_C when the chamber is open.

If, in the absence of an incoming wave, the chamber is subjected to an imposed excess pressure $p_e(t) = p_0\exp(i\omega t)$ causing a chamber wave $\tilde{\eta}_C(x,y)\exp(i\omega t)$, the admittance Z of the system is defined by the equation

$$Z = -i\omega A_C(g\rho)^{-1}\langle\tilde{\eta}_C(x,y)\rangle/\eta_p, \tag{3.2}$$

where $A_C = ab$ is the surface area of the chamber, g is the acceleration due to gravity, ρ is the water density, and $\eta_p = p_0/g\rho$ is the wave-amplitude equivalent of the pressure amplitude p_0. When convenient, we separate the admittance into its real and imaginary parts by writing $Z = B + i\omega A$.

In an actual working situation the system is subjected to an incoming wave with amplitude η_0, and the resulting wave amplitude $\eta_C(x,y)$ and the excess-pressure amplitude p_C in the chamber depend on the turbine constant C_t. In large-scale wave-power plants air compressibility will have a noticeable effect on the performance. In this respect, it is shown in Appendix A that, in a first approximation consistent with linear wave theory, the compressibility of air can be taken into account by the introduction of an effective turbine constant $\Lambda = C_t + i\omega\Delta$, where $\Delta = V_C/\kappa p_a$. Here $V_C = A_C H$ is the chamber volume, p_a is the atmospheric pressure, and $\kappa = 1.4$ on the assumption of adiabaticity.

The amplitude ratio ξ_C and pressure ratio $\pi_C = p_C/\eta_0$ can then be expressed in terms of ξ_0, Z and Λ by the equations

$$\left.\begin{aligned}\xi_C &= \xi_0\Lambda(\Lambda+Z)^{-1}, \\ \pi_C &= i\omega A_C\xi_0(\Lambda+Z)^{-1}.\end{aligned}\right\} \tag{3.3}$$

The pressure ratio in a closed chamber ($C_t = 0$) is thus $\pi_1 = i\omega A_C\xi_0(Z+i\omega\Delta)^{-1}$. Note, furthermore, that owing to the air compressibility an infinitely large chamber ($\Delta\to\infty$) is equivalent to an open chamber ($C_t\to\infty$) of finite size; in both cases $\xi_C\to\xi_0$ and $\pi_C\to 0$.

Writing the mean power absorbed by the system as $P|\eta_0|^2$, we can express the power ratio as

$$\begin{aligned}P &= \tfrac{1}{4}A_C[(i\omega\xi_C)^*\pi_C + \pi_C^*(i\omega\xi_C)], \\ &= \tfrac{1}{2}\mathrm{Re}(\Lambda)|\pi_C|^2.\end{aligned} \tag{3.4}$$

Another useful measure of the performance of the system is the capture width w, where

$$\left.\begin{aligned} w &= P/J, \\ J &= \frac{g^2\rho}{4\omega} f(kh), \\ f(kh) &= \left[1+\frac{2kh}{\sinh 2kh}\right]\tanh kh, \end{aligned}\right\} \tag{3.5}$$

in which k is the wavenumber and $J|\eta_0|^2$ is the power per unit width in the incident wave. Equivalent dimensionless quantities are the capture-width ratio

$$W = w/b \tag{3.6}$$

and, for an absorber in a channel, the efficiency

$$E = w/c. \tag{3.7}$$

For a given system geometry and wave frequency the turbine constant C_t can be used to optimize the absorbed power. In terms of W, the optimum situation corresponds to a value

$$W_{\max} = (2g^2\rho)^{-1} \frac{A_C^2 \omega^3}{b} \frac{|\xi_0|^2}{f(kh)} B^{-1}, \tag{3.8}$$

which occurs for $\Delta = Z^*$, implying a phase lag between the flux through the turbine and the driving pressure. If no such phase lag is present, i.e. if the turbine constant C_t is real, we obtain an optimum capture-width ratio $W'_{\max}$ by choosing C_t equal to C_0, where

$$\left.\begin{aligned} \frac{W'_{\max}}{W_{\max}} &= 4BC_0[(C_0+B)^2+\omega^2(A+\Delta)^2]^{-1}, \\ C_0 &= [B^2+\omega^2(A+\Delta)^2]^{\frac{1}{2}}. \end{aligned}\right\} \tag{3.9}$$

We note that $W_{\max}$ and $W'_{\max}$ coincide at frequencies for which $A+\Delta = 0$.

4. Wave amplitude

In the present chapter we address the problem of calculating the quantity ξ_0. In other words, we consider the situation where the system in figure 1 is subjected to an incident wave $\hat{\eta}_i(x,t) = \eta_i(x)\exp(i\omega t)$ travelling towards the open end of the absorber, where $\eta_i(x) = \eta_0 \exp(ikx')$, and calculate the corresponding average wave amplitude in the open chamber.

The velocity potential in the various regions of the system can be expressed in terms of the eigenmodes consistent with the boundary conditions on the solid walls and on the surface and the bottom of the sea. Using the indices q and n to denote transverse modes (y-dependence) and vertical modes (z-dependence) respectively, we can write the velocity potential ϕ and wave amplitude η in the front region 1 as

$$\left.\begin{aligned} \phi_1(x,y,z) &= \frac{ig}{\omega}\sum_n \eta_{1n}(x,y)\, e_n(z), \\ \eta_1(x,y) &= \sum_n \eta_{1n}(x,y), \end{aligned}\right\} \tag{4.1}$$

where

$$\eta_{1n}(x,y) = \eta_0[\exp(\mathrm{i}kx')\,\delta_{n0} + \sum_q a_{1nq}\exp(-\nu_{nq}x')\,V_q(y)]. \tag{4.2}$$

In principle, the summation indices q and n range from zero to infinity, and the coefficients a_{1nq} are as yet unknown. Furthermore,

$$\left.\begin{aligned} \nu_{0q} &= \begin{cases} \mathrm{i}\left[k^2-\left(\frac{2\pi q}{c}\right)^2\right]^{\frac{1}{2}} & \left(q<\frac{c}{\lambda}\right), \\ \left[\left(\frac{2\pi q}{c}\right)^2-k^2\right]^{\frac{1}{2}} & \left(q>\frac{c}{\lambda}\right), \end{cases} \\ \nu_{nq} &= \left[m_n^2+\left(\frac{2\pi q}{c}\right)^2\right]^{\frac{1}{2}} \quad (n>0), \\ V_q(y) &= \cos\frac{2\pi qy}{c}, \quad \lambda = \frac{2\pi}{k}. \end{aligned}\right\} \tag{4.3}$$

We refer to Appendix B regarding the definitions of the eigenfunctions $e_n(z)$ and eigenvalues m_n for the z-dependence; note, in particular, that $m_0 = \mathrm{i}k$ and $e_n(0) = 1$. We emphasize that a reflected-wave component $\eta_{1r}(x) = \eta_0 a_{100}\exp(-\mathrm{i}kx')$ is contained in (4.2).

Considering for the time being the case where the side regions between the absorber and the channel walls are accessible, we can, similarly, write the contribution from the mode n to the wave amplitude in the back region 3 as

$$\left.\begin{aligned} \eta_{3n}(x,y) &= \eta_0 \sum_q a_{3nq}\exp(\nu_{nq}x'')\,V_q(y), \\ x'' &= x'+l' = x+a, \quad l' = a+l, \end{aligned}\right\} \tag{4.4}$$

where the transmitted wave is $\eta_{3t}(x) = \eta_0 a_{300}\exp(\mathrm{i}kx'')$. The side regions 2 contain waves travelling both up and down the channel, and the relevant width parameter is there $c' = c-b$. Thus

$$\left.\begin{aligned} \eta_{2n}(x,y) &= \eta_0 \sum_q [a_{2nq}\exp(\epsilon_{nq}x') + b_{2nq}\exp(-\epsilon_{nq}x')]\,w_q(y), \\ w_q(y) &= \cos\{2\pi q[|y|-\tfrac{1}{2}b]/c'\}, \end{aligned}\right\} \tag{4.5}$$

where the expressions for ϵ_{nq} are obtained from those for ν_{nq} by a substitution of c' for c.

We now turn our attention to the internal regions of the absorber. Looking again at an arbitrary z-mode n, we can write the wave amplitude in the chamber region as

$$\left.\begin{aligned} \eta_{Cn}(x,y) &= \eta_0 \sum_q a_{nq}\cosh(\gamma_{nq}x'')\,v_q(y), \\ v_q(y) &= \cos(2\pi qy/b), \end{aligned}\right\} \tag{4.6}$$

where we obtain γ_{nq} from the expressions for ν_{nq} by substituting b for c, and where the x-dependence of the wave amplitude (4.6) follows from the boundary condition $\partial\phi/\partial x = 0$ at the back wall ($x'' = 0$). Also, in the harbour region we are concerned with a linear combination of waves along the positive and negative x-axes. We note, however, that at $x = 0$ the derivative $\partial\phi/\partial x$ should be the same on both sides of the

barrier (in particular, $\partial\phi/\partial x = 0$ for $-d < z < 0$). The harbour wave amplitude can then be written as

$$\eta_{\mathrm{H}n}(x,y) = \eta_0 \sum_q [a_{nq} \cosh \gamma_{nq} x'' + b_{nq} \cosh \gamma_{nq} x] v_q(y), \tag{4.7}$$

where the coefficients b_{nq} define the difference in wave amplitude between the two sides of the barrier.

We note at this point that only the coefficients a_{n0} enter explicitly into the expression for the mean chamber amplitude,

$$\xi_0 = \sum_n a_{n0} \frac{\sinh m_n a}{m_n a}. \tag{4.8}$$

However, the various unknown coefficients that we have introduced are interrelated through the matching conditions for the velocity potential and its derivative with respect to x at the boundaries between the various regions. For example, at the barrier the chamber and harbour potentials ϕ_{C} and ϕ_{H}, which for $x = 0$ already fulfil the condition $\partial\phi_{\mathrm{H}}/\partial x = \partial\phi_{\mathrm{C}}/\partial x$ at any y and z, should satisfy the requirements $\partial\phi_{\mathrm{C}}/\partial x = 0$ for $-d < z < 0$ and $\phi_{\mathrm{H}} = \phi_{\mathrm{C}}$ for $-h < z < d$. In integrated form this gives a set of linear equations for the coefficients a_{nq} and b_{nq}; these equations couple the various vertical modes n but not the transverse modes q.

At present, however, we find it more instructive to consider the limiting case of zero barrier depth, i.e. the case where the potentials in the harbour and open chamber are described by the same expression, corresponding to $b_{nq} = 0$ in (4.7). We shall return to the influence of the barrier depth in §7.

For $d = 0$ the only vertical mode that is present in the system is $n = 0$, since the incident wave contains just this mode, and all solid walls extend down to the sea bed. For purposes of the subsequent admittance calculation it is nevertheless convenient to pretend not to know this off-hand and derive linear equations for the coefficients in any mode n. These equations then couple different transverse modes q but leave the vertical modes n uncoupled. Explicitly, the required matching conditions can be written as

$$\left.\begin{aligned}
&\phi_{\mathrm{H}} = \phi_1 \quad (x' = 0,\ 0 < y < \tfrac{1}{2}b),\\
&\phi_2 = \phi_1 \quad (x' = 0,\ \tfrac{1}{2}b < y < \tfrac{1}{2}c),\\
&\phi_2 = \phi_3 \quad (x'' = 0,\ \tfrac{1}{2}b < y < \tfrac{1}{2}c),\\
&\frac{\partial\phi_1}{\partial x} = \begin{cases} \dfrac{\partial\phi_{\mathrm{H}}}{\partial x} & (x' = 0,\ 0 < y < \tfrac{1}{2}b),\\ \dfrac{\partial\phi_2}{\partial x} & (x' = 0,\ \tfrac{1}{2}b < y < \tfrac{1}{2}c), \end{cases}\\
&\frac{\partial\phi_3}{\partial x} = \begin{cases} 0 & (x'' = 0,\ 0 < y < \tfrac{1}{2}b),\\ \dfrac{\partial\phi_2}{\partial x} & (x'' = 0,\ \tfrac{1}{2}b < y < \tfrac{1}{2}c). \end{cases}
\end{aligned}\right\} \tag{4.9}$$

In practice, our expansions of the velocity potential in the various regions will of course be limited to a finite number of terms. We could, for example, attempt to determine the corresponding coefficients by a least-squares method. As indicated

above, however, we can instead obtain a set of linear equations for the coefficients by integrating (4.9) over appropriate regions of the transverse coordinate y. Roughly speaking, we are then simply expressing Fourier coefficients as integrals over the function to be expanded.

If we now limit the order q of the transverse modes that we consider to a maximum value Q in the harbour and chamber, and to maximum values Q_1, Q_2 and Q_3 in the respective external regions, we have $Q+Q_1+2Q_2+Q_3+5$ unknown coefficients a_{nq}, a_{1nQ}, a_{2nQ}, b_{2nQ} and a_{3nQ}, which should satisfy the equations

$$\left.\begin{aligned}
&\tfrac{1}{2}(\delta_{Q0}+1)\,a_{nq}\cosh\gamma_{nq}l'-\sum_{q'=0}^{Q_1}A_{q'q}a_{1nq'}-C_{nq},\quad q=0,1,\ldots,Q,\\
&\tfrac{1}{2}(\delta_{Q0}+1)\,(a_{2nq}+b_{2nq})-\sum_{q'=0}^{Q_1}B_{q'q}a_{1nq'}=D_{nq},\quad q=0,1,\ldots,Q_2,\\
&\tfrac{1}{2}(\delta_{Q0}+1)\,[a_{2nq}\exp(-\epsilon_{nq}l')+b_{2nq}\exp(\epsilon_{nq}l')]-\sum_{q'=0}^{Q_3}B_{q'q}a_{3nq'}=E_{nq},\\
&\qquad\qquad q=0,1,\ldots,Q_2,\\
&\tfrac{1}{2}(\delta_{Q0}+1)\,\nu_{nq}a_{1nq}+\frac{b}{c}\sum_{q'=0}^{Q}\gamma_{nq'}A_{qq'}a_{nq'}\sinh\gamma_{nq'}l'\\
&\qquad\qquad+\frac{c'}{c}\sum_{q'=0}^{Q_2}\epsilon_{nq'}B_{qq'}(a_{2nq'}-b_{2nq'})=F_{nq},\quad q=0,1,\ldots,Q_1,\\
&\tfrac{1}{2}(\delta_{Q0}+1)\,\nu_{nq}a_{3nq}-\frac{c'}{c}\sum_{q'=0}^{Q_2}\epsilon_{nq'}B_{qq'}[a_{2nq'}\exp(-\epsilon_{nq'}l')\\
&\qquad\qquad-b_{2nq'}\exp(\epsilon_{nq'}l')]=G_{nq},\quad q=0,1,\ldots,Q_3.
\end{aligned}\right\}\tag{4.10}$$

We have here

$$\left.\begin{aligned}
&A_{0q}=B_{0q}=\delta_{q0},\\
&A_{q'q}=\begin{cases}(-1)^{q+1}\left(\dfrac{bq'}{c}\right)^2\left[q^2-\left(\dfrac{bq'}{c}\right)^2\right]^{-1}a_{q'} & \left(q\neq\dfrac{bq'}{c}\right),\\[2ex] \dfrac{1}{2} & \left(q=\dfrac{bq'}{c}\right),\end{cases}\qquad(q'\neq 0)\\
&B_{q'q}=\begin{cases}\dfrac{b}{c'}\left(\dfrac{c'q'}{c}\right)^2\left[q^2-\left(\dfrac{c'q'}{c}\right)^2\right]^{-1}a_{q'} & \left(q\neq\dfrac{c'q'}{c}\right),\\[2ex] \tfrac{1}{2}(-1)^{q'+q} & \left(q=\dfrac{c'q'}{c}\right)\end{cases}\\
&a_{q'}=\frac{\sin(\pi q'b/c)}{\pi q'b/c},
\end{aligned}\right\}\tag{4.11}$$

and

$$\left.\begin{aligned}
&C_{nq}=D_{nq}=(\mathrm{i}k)^{-1}F_{nq}=\delta_{n0}\delta_{q0},\\
&E_{nq}=G_{nq}=0.
\end{aligned}\right\}\tag{4.12}$$

The appearance of the factor δ_{n0} in (4.12) then makes all coefficients zero for $n\neq 0$, and the $d=0$ average chamber amplitude is thus simply $\xi_0=a_{00}(\sin ka)/ka$.

By making appropriate changes in (4.10) or (4.12), we can now cover several other situations as well.

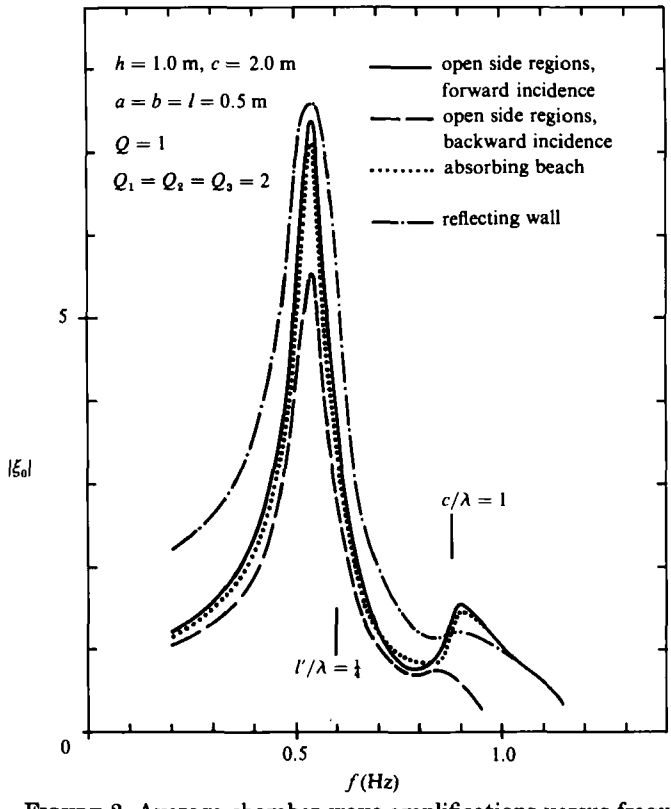

FIGURE 2. Average chamber-wave amplifications versus frequency.

(1) *Backward incidence*

The incident wave $\eta_0 \exp(-ikx')$ is in this case travelling towards the closed end of the absorber; this amounts to a replacement of the driving terms (4.12) by

$$\left.\begin{aligned} E_{nq} &= -(ik)^{-1} G_{nq} = \exp(ikl')\,\delta_{n0}\,\delta_{q0}, \\ C_{nq} &= D_{nq} = F_{nq} = 0. \end{aligned}\right\} \tag{4.13}$$

(2) *Absorbing beach*

We assume in this case forward incidence, but a situation where no waves are reflected back into region 2 at the far end of the absorber. This is achieved if region 2 contains an absorbing beach at the level of or behind the mouth of the harbour. In our mathematical model we put $b_{2nq} = a_{3nq} = 0$ and omit those equations in (4.10) that contain $\exp(\pm\epsilon_{nq} l')$.

(3) *Reflecting wall*

The side regions of the channel are now closed by a totally reflecting wall at $x' = 0$. As far as (4.10) is concerned, we put $b_{2nq} = a_{2nq}$ and $a_{3nq} = 0$, and again omit the equations containing $\exp(\pm\epsilon_{nq} l')$.

Figure 2 shows the resulting average wave amplification $|\xi_0|$ on the open chamber for a specific geometry in model scale, for forward and backward incidence onto a system with open side regions as well as for the systems with an absorbing beach or

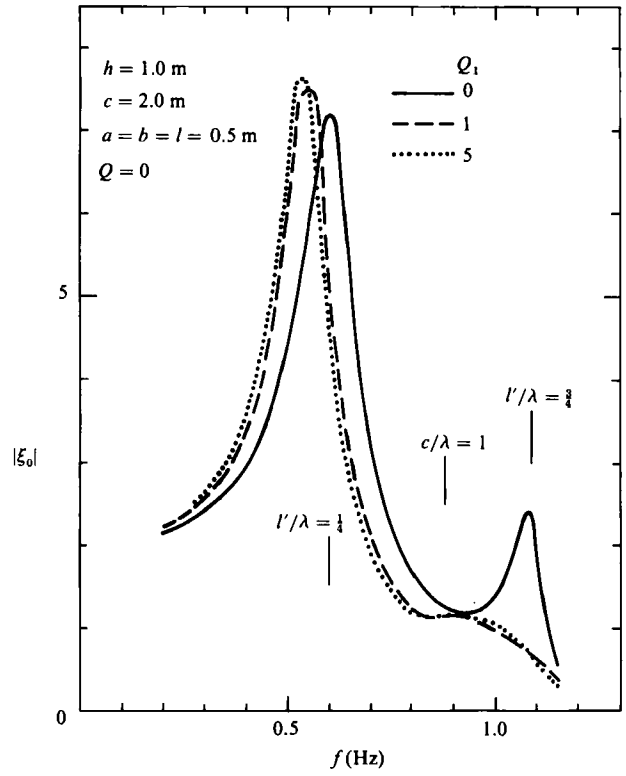

FIGURE 3. The influence of transverse channel modes on the average chamber-wave amplification for an absorber in a reflecting wall.

a reflecting wall. In this and subsequent figures we use $f = \omega/2\pi$ (in Hz) as the frequency variable. While the angular frequency ω is the more convenient variable in the mathematical expressions, the frequency f or its inverse, the period, seems preferable from a physical point of view. Qualitatively, the frequency dependence of $|\xi_0|$ is much the same in all the four cases we consider, and, not unexpectedly, the main peak can roughly be interpreted as a quarter-wave resonance in the total length $l' = l + a$ of the absorber. Note also the behaviour in the region where the wavelength λ matches the width c of the channel.

The number of transverse modes needed to give an acceptable description of the wave picture in the various regions of course depends on the frequency. In the frequency range covered by figure 2 we expect the transverse modes $q \geqslant 1$ in the harbour and chamber to be rather unimportant, since with the present geometry the matching point $\lambda = b$ appears at $f = 1.77$ Hz. This is indeed confirmed by the numerical calculations, the influence of the internal $q \geqslant 1$ modes on the values of $|\xi_0|$ in figure 2 being on the 1 % level or less.

The situation is different for the external transverse modes, because in the present example $\lambda = c$ already at $f = 0.88$ Hz. This is demonstrated in figure 3, which shows $|\xi_0|$ in the reflecting-wall case for $Q_1 = 0$, 1 and 5. We see that the external $q = 1$ mode has a very noticeable effect on the wave amplification, in that it moves and enhances the quarter-wave and all but destroys the three-quarter-wave resonance. On the other hand, it then makes little difference if we increase Q_1 from 1 to 5. Similarly, when the side regions are open we can investigate the influence of the upper

limits Q_2 and Q_3 for the transverse modes at the sides and back of the absorber. All told, in the frequency range we are considering, the values $Q = 1$, $Q_1 = Q_2 = Q_3 = 2$ used in figure 2 and subsequent figures describe the actual situation very well.

Let us now look at the low-frequency limit where no modes other than $q = 0$ are present to an appreciable degree in any part of the system, i.e. put $Q = Q_1 = Q_2 = Q_3 = 0$. The set (4.10) is then reduced to five equations for equally many unknown coefficients. Using the indices + and − to indicate forward and backward incidence onto a system with freely accessible side regions 2, we obtain the average chamber amplitudes

$$\left.\begin{aligned} \xi_{0+} &= [(1-\mu)\cos kl' + \mathrm{i}\sin kl']\,\zeta\,\frac{\sin ka}{ka}, \\ \xi_{0-} &= (1-\mu)\exp(\mathrm{i}kl')\,\zeta\,\frac{\sin ka}{ka}, \end{aligned}\right\} \tag{4.14}$$

where $\mu = b/c$ and

$$\zeta = \{1-\mu+[1-\tfrac{1}{2}\mu]\,\mathrm{i}\sin(kl')\exp(\mathrm{i}kl')\}^{-1}. \tag{4.15}$$

For the case of an absorbing beach (index b) or reflecting wall (index w) we have just three unknown coefficients, and

$$\left.\begin{aligned} \xi_{0\mathrm{b}} &= [\cos kl' - \tfrac{1}{2}\mu\exp(-\mathrm{i}kl')]^{-1}\,\frac{\sin ka}{ka}, \\ \xi_{0\mathrm{w}} &= 2[\cos kl' + \mathrm{i}\mu\sin kl']^{-1}\,\frac{\sin ka}{ka}. \end{aligned}\right\} \tag{4.16}$$

As the width ratio μ approaches zero these expressions all give $\xi_0 \propto [\cos kl']^{-1}$, in agreement with the interpretation of the peak as a quarter-wave resonance.

5. Admittance

If the chamber is subjected to a periodic excess pressure with amplitude $p_0 = g\rho\eta_\mathrm{p}$ the corresponding velocity potential $\tilde{\phi}_\mathrm{C}$ and wave amplitude $\tilde{\eta}_\mathrm{C}$ can be written

$$\left.\begin{aligned} \tilde{\phi}_\mathrm{C}(x,y,z) &= \frac{\mathrm{i}g}{\omega}\,[\sum_n \tilde{\eta}_{\mathrm{C}n}(x,y)\,e_n(z) + \eta_\mathrm{p}], \\ \tilde{\eta}_{\mathrm{C}n}(x,y) &= \eta_\mathrm{p}\sum_q a_{nq}\cosh(\gamma_{nq}x'')\,v_q(y). \end{aligned}\right\} \tag{5.1}$$

According to (3.2), the admittance of the system is then

$$Z = -\mathrm{i}\omega A_\mathrm{C}(g\rho)^{-1}\sum_{n=0}^{N} a_{n0}\,\frac{\sinh m_n a}{m_n a}, \tag{5.2}$$

where a finite number $N+1$ of vertical modes has been included.

For the other parts of the system we can use the same expressions for the velocity potential and wave amplitudes as in §4, except that η_0 is replaced by η_p. By matching potentials and derivatives at the various boundaries we can again obtain a set of linear equations of the type (4.10) for the unknown coefficients. We recall from §4 that in the limiting case $d = 0$ only the mode $n = 0$ contributes to the wave amplitude. For the admittance this is not the case; nevertheless, also now an important simplification occurs for $d = 0$, viz the fact that the different n-modes are uncoupled. In fact, it turns

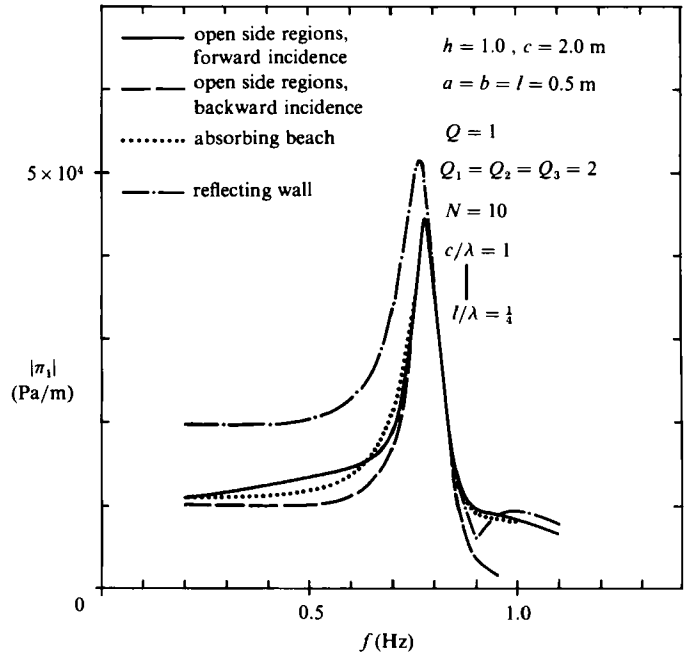

FIGURE 4. Closed-chamber pressure ratios versus frequency.

out that for $d = 0$ the coefficients that determine the admittance can be obtained by using the right-hand sides

$$\left.\begin{aligned} C_{nq} &= g_n(0)\cosh(m_n l)\,\delta_{q0}, \\ F_{nq} &= \mu m_n g_n(0)\sinh(m_n l)\,A_{q0}, \\ D_{nq} &= E_{nq} = G_{nq} = 0 \end{aligned}\right\} \tag{5.3}$$

in (4.10), rather than (4.12) or (4.13). The integrals g_n are defined in Appendix B, (B 7).

The admittance is of course not affected by the direction of incidence of the incoming wave; through the matching conditions we have accounted for waves radiated both up and down the channel. The absorbing-beach and reflecting-wall cases can be treated as in §4, i.e. by a change in the left-hand sides of (4.10) and a reduction in the number of equations.

Instead of giving numerical examples showing the frequency dependence of the admittance, we consider the pressure ratio $|\pi_1|$ in a closed chamber when the system is subjected to an incoming wave. We shall as in §4 be concerned with model-scale systems, where the effects of air compressibility are unappreciable. Figure 4 applies to the same geometry as in figure 2 and supports the intuitive physical picture in which a quarter-wave resonance in the *harbour* manifests itself as a pressure resonance in the chamber. However, in figure 4 the frequency where $l = \frac{1}{4}\lambda$ coincides with that where $c = \lambda$, and we refer to figure 5 for a case where the transverse matching point $c = \lambda$ is outside the frequency range under consideration. The pressure ratio is shown for two finite harbour lengths l as well as for $l = 0$, and it is seen that for the longest harbour even a three-quarter-wave resonance appears within the bounds of the figure.

As in the previous chapter we take a closer look at the low-frequency range, where only the transverse mode $q = 0$ need be considered. We note that all z-modes other

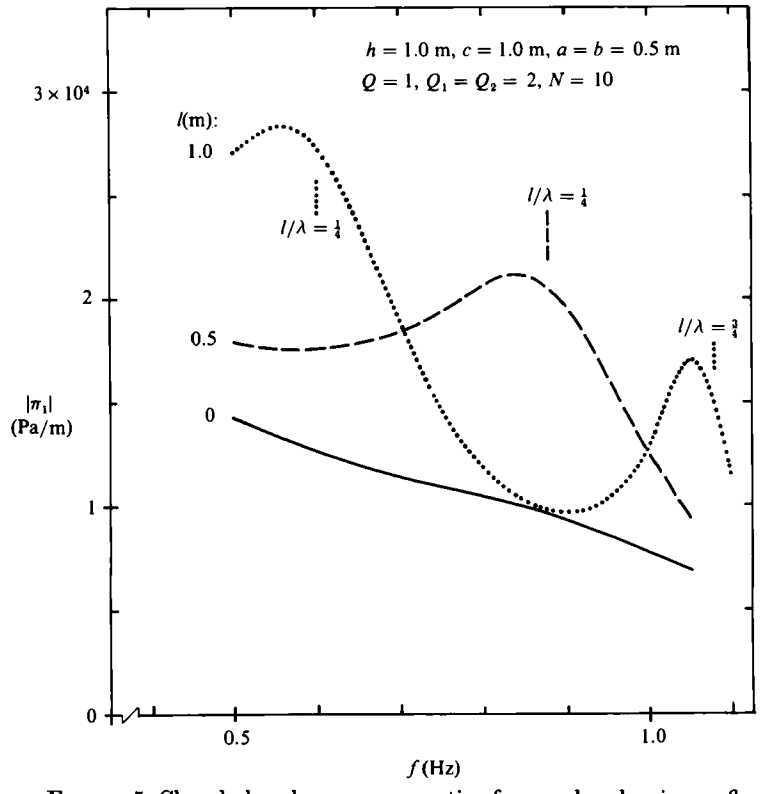

FIGURE 5. Closed-chamber pressure ratios for an absorber in a reflecting wall versus frequency for various harbour lengths.

than $n = 0$ contribute solely to the imaginary part of the admittance. The linear equations at $n = 0$ thus determine the real part B of the admittance completely, and we find that, for the systems with open side regions, an absorbing beach and a reflecting wall, the appropriate $d = 0$ low-frequency expressions can be written respectively as

$$\left.\begin{aligned} B_{\pm} &= 2B_0\{(1-\mu)^2+\mu[1-\tfrac{1}{2}\mu]\sin^2 kl'\}\,|\zeta|^2\left[\frac{\sin ka}{ka}\right]^2,\\ B_{\mathrm{b}} &= 2B_0[1-\tfrac{1}{2}\mu]\,|\xi_{0\mathrm{b}}|^2,\\ B_{\mathrm{w}} &= B_0\,|\xi_{0\mathrm{w}}|^2,\\ B_0 &= (2g^2\rho)^{-1}\frac{A_{\mathrm{C}}^2\omega^3}{c}\,[f(kh)]^{-1}, \end{aligned}\right\} \tag{5.4}$$

where $f(kh)$ is defined in (3.5) and ζ in (4.15).

Note also that

$$B_{\pm} = B_0(|\xi_{0+}|^2+|\xi_{0-}|^2), \tag{5.5}$$

which is the equivalent of the relation (A 33) in Evans (1982*a*).

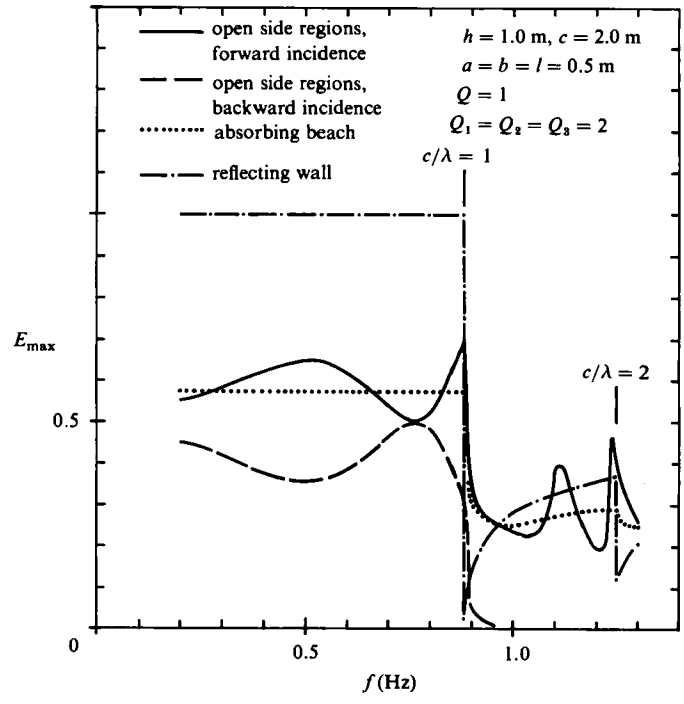

FIGURE 6. Optimum efficiencies versus frequency.

6. Performance

In §§4 and 5 we have indicated how the system parameters ξ_0 and Z can be found for given geometrical parameters and frequency. If we further specify the turbine constant C_t the absorbed power can then be calculated from the formulae in §3.

In terms of the efficiency $E = w/c = \mu W$ the optimum performance of the system is, according to (3.8), given by $E_{\max} = (B_0/B)\,|\xi_0|^2$, where B is the real part of Z and B_0 is defined in (5.4). Figure 6 shows the optimum efficiencies for the same geometry as in figures 2 and 4, and we note the abrupt changes in performance at the transverse matching point $\lambda = c$. These discontinuities are similar to those observed by Srokosz (1980) for an oscillating body in an infinitely deep canal.

We can obtain simple expressions for $E_{\max}$ by using the expressions (4.14), (4.15) and (5.4) corresponding to $Q = Q_1 = Q_2 = Q_3 = 0$. For an absorber in a reflecting wall or an absorbing beach the resulting optimum efficiencies are exact for all wavelengths larger than the channel width c, although the separate values for ξ_0 and B depend on the number of transverse modes included. For the four cases that we have looked at, viz open side regions with forward or backward incidence, absorbing beach and reflecting wall, the optimum efficiencies in question are

$$\left.\begin{aligned} &E_{\max+} = \tfrac{1}{2}\{(1-\mu)^2 + 2\mu[1-\tfrac{1}{2}\mu]\sin^2 kl'\}\{(1-\mu)^2 + \mu[1-\tfrac{1}{2}\mu]\sin^2 kl'\}^{-1}, \\ &E_{\max-} = 1 - E_{\max+}, \quad E_{\max\,b} = (2-\mu)^{-1}, \quad E_{\max\,w} = 1. \end{aligned}\right\} \tag{6.1}$$

For $\mu \to 0$ we obtain the point-absorber result $E_{\max+} = E_{\max-} = E_{\max\,b} = \frac{1}{2}$, whereas $E_{\max\,w}$ is always twice that value due to the presence of the reflected wave from the wall. As a check on the results note also that when the absorber occupies the whole width of the channel ($\mu = 1$) $E_{\max+} = E_{\max\,b} = E_{\max\,w} = 1$, $E_{\max-} = 0$.

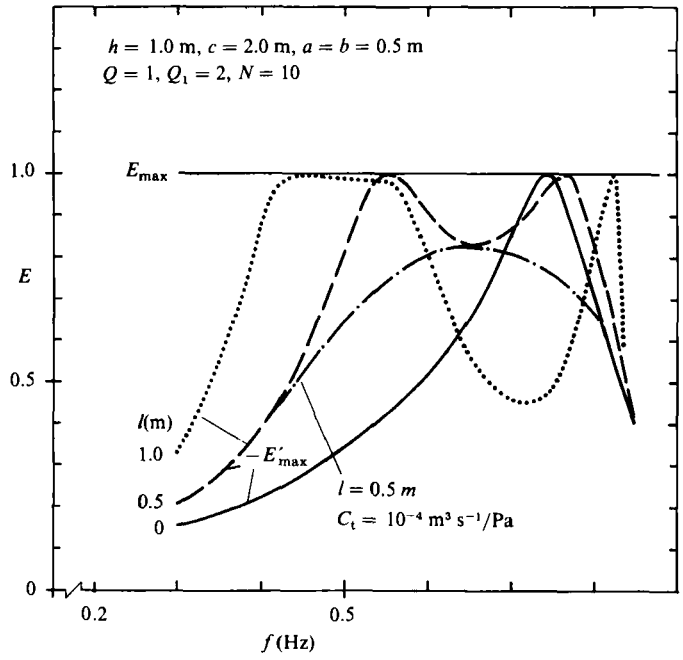

FIGURE 7. Optimum efficiencies for an absorber in a reflecting wall versus frequency for various harbour lengths.

The absorbing-beach result is identical with that obtained by Evans (1982*b*) for a long absorber. However, the main basis for this result is the assumption that no waves are travelling upstream through the side regions; in Evans' case this is then implicitly assumed through the use of expressions applicable to a semi-infinite duct. For an absorber in a channel with open side regions the boundary conditions have the consequence that $E_{\max}$ is dependent on the length of the absorber, the relevant parameter being $\sin^2 kl'$, where $l' = l+a$. For a given width ratio $0 < \mu < 1$ and wavelength $\lambda = 2\pi/k$ the largest and smallest values that can be obtained for $E_{\max+}$ by variation of l' are, according to (6.1),

$$\left.\begin{aligned} E^{(\max)}_{\max+} &= \tfrac{1}{2}[1-\mu+\tfrac{1}{2}\mu^2]^{-1} \quad (l' = (m+\tfrac{1}{2})\lambda/2), \\ E^{(\min)}_{\max+} &= \tfrac{1}{2} \qquad\qquad\qquad\quad (l' = m\lambda/2), \end{aligned}\right\} \quad m = 0, 1, \ldots. \tag{6.2}$$

Turning now to the optimum efficiency $E'_{\max}$ corresponding to a real turbine constant C_t, we note that even for an absorber in a reflecting wall or an absorbing beach $E'_{\max}$ depends on the separate lengths of the chamber and the harbour, since these lengths influence the imaginary part of the admittance. Figure 7 shows examples of how the frequency dependence of $E'_{\max}$ changes as one varies the harbour length l but keeps all other geometrical parameters constant. For one harbour length we also show the efficiency E for a certain fixed value of C_t. In figure 7, as in the subsequent numerical examples in this section, we limit ourselves to the case of an absorber in a reflecting wall; in particular, figure 8 shows $E'_{\max}$ for various widths b of an absorber without a harbour.

A real-life wave-power station is of course subjected to waves of varying amplitude, direction, frequency and phase. The problem of cost optimization of such systems for given wave climates and power requirements is beyond the scope of the present

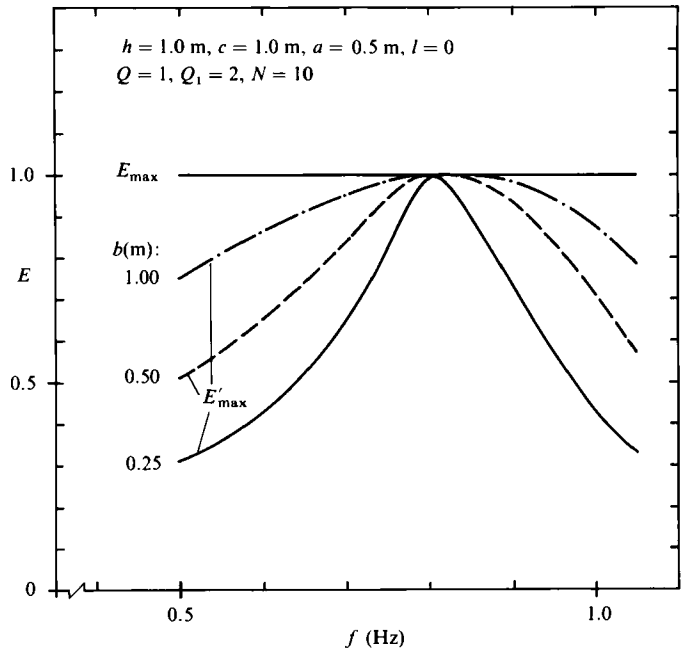

FIGURE 8. Optimum efficiencies for an absorber in a reflecting wall versus frequency for various absorber widths.

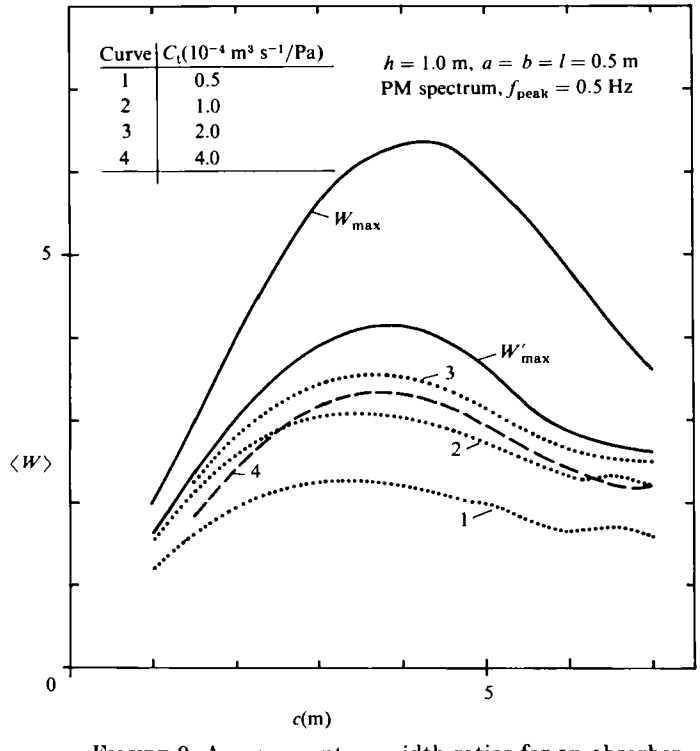

FIGURE 9. Average capture-width ratios for an absorber in a reflecting wall versus channel width.

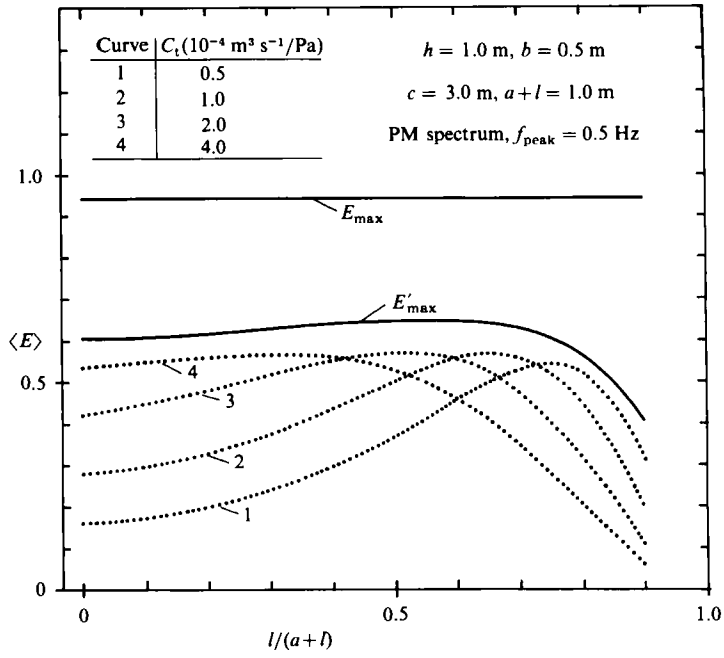

FIGURE 10. Average efficiencies for an absorber in a reflecting wall versus the ratio of harbour length to total absorber length.

paper. But let us at least look at some typical frequency averages for the power absorbed by a model-scale water column. In these examples the incident power is distributed according to a Pierson–Moskowitz spectrum peaking at 0.5 Hz.

In figure 9 we keep the absorber geometry constant and vary the channel width c; this is equivalent to varying the distance between the units in an infinite row of absorbers. When c is varied and b kept constant the relevant parameter is the capture-width ratio W. As far as the average W_{max} and W'_{max} are concerned, we have assumed that the turbine constant is optimized, but in the case of W'_{max} kept real, at each frequency; the other curves correspond to fixed and real values of C_t. Figure 10 shows another type of frequency average. The distance between the absorbers is kept constant, as is the width and total length $l' = l+a$ of each absorber. What is varied is the ratio of harbour length l to total length l', and the figure shows the optimum average efficiencies E_{max} and E'_{max} as well as the curves corresponding to the same fixed values of C_t as in figure 9.

It is clear from these figures that a lot of thought should be given to the specifications for any actual wave-power installation, not least because the choice of turbine may have a major influence on the total cost. Roughly speaking, a reduction in the required value of C_t means a turbine that is smaller in diameter and cheaper to manufacture. In this respect, figure 10 suggests that a long harbour and short chamber might give considerable savings in turbine costs as compared with a short harbour and correspondingly long chamber.

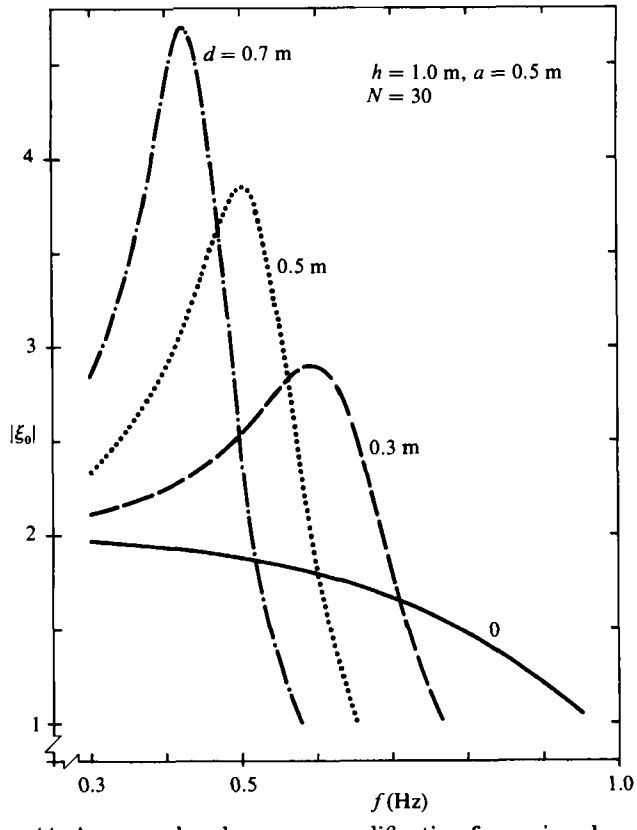

FIGURE 11. Average chamber-wave amplification for various barrier depths.

7. Finite barrier depth

The calculations presented in the previous sections apply to the limiting case of zero barrier depth d. For finite d we have a coupling between the various vertical modes n, in addition to the coupling that we have seen between the transverse modes q. To avoid the latter complication we shall for the present limit ourselves to the case of an absorber which occupies the whole width of the channel.

By requiring that the derivative $\partial\phi/\partial x$ is zero on the barrier and that ϕ as well as $\partial\phi/\partial x$ is continuous under the barrier we can again obtain linear equations which determine the coefficients a_n describing the wave motion in the chamber. If we include $N+1$ vertical modes n these equations can be written

$$\left.\begin{aligned} &\sum_{n'=0}^{N}\left\{f_{n'}e_{nn'}(d)+\frac{1}{2}\frac{m_{n'}}{m_n}[\delta_{nn'}-e_{nn'}(d)]\right\}\tilde{a}_{n'}=C_n,\\ &\tilde{a}_n=a_n\sinh m_n a,\quad f_n=[1-\exp(-2m_n a)]^{-1},\\ &\qquad n=0,1,\ldots,N. \end{aligned}\right\} \tag{7.1}$$

For an incoming wave $\eta_0\exp(ikx)$ we have

$$\left.\begin{aligned} C_n &= e_{n0}(d),\\ \xi_0 &= \sum_{n=0}^{N} a_n\frac{\sinh m_n a}{m_n a}, \end{aligned}\right\} \tag{7.2}$$

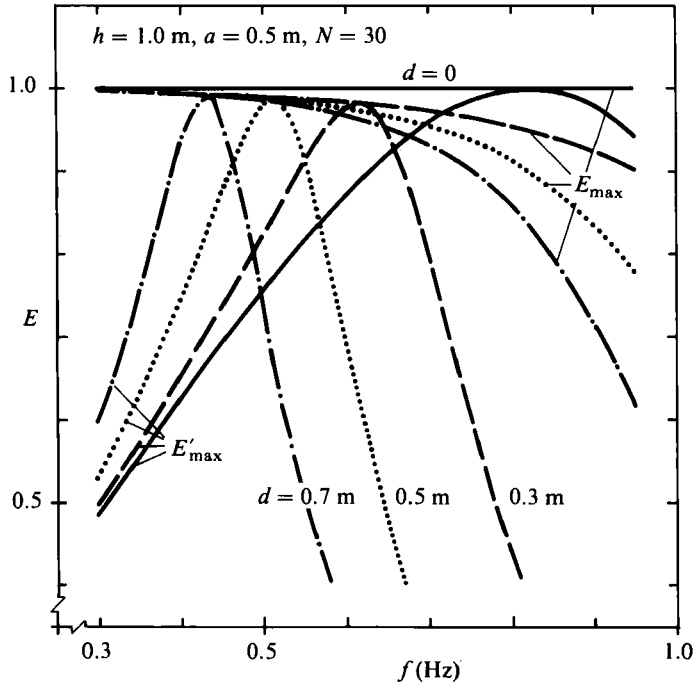

FIGURE 12. Optimum efficiencies for various barrier depths in the case $b = c$.

and for the admittance calculation

$$C_n = \tfrac{1}{2}g_n(d), \quad \bar{Z} = \mathrm{i}\omega a(g\rho)^{-1} \sum_{n=0}^{N} a_n \frac{\sinh m_n a}{m_n a}, \tag{7.3}$$

where $\bar{Z} = Z/b = Z/c$ is the admittance per unit width. The integrals $e_{nn'}$ and g_n are defined in Appendix B.

Figure 11 shows an example of how the frequency dependence of the chamber amplitude changes as the barrier depth is increased. The real part of the admittance depends in a similar way on d, with the result that the optimum efficiency $E_{\max}$ displayed in figure 12 depends much more weakly on the barrier depth than might be inferred from the behaviour of $|\xi_0|$. However, it is also seen from figure 12 that $E'_{\max}$, which corresponds to a turbine air flux in phase with the driving pressure, again depends quite strongly on d.

A situation equivalent to our $b = c$ case was studied by Falcão & Sarmento (1980) for $d = 0$, and by complex-variable techniques a formal solution was obtained also for finite barrier depth. For $d = 0$ and infinite water depth h these authors find that the resonance point where $E'_{\max} = E_{\max}$ should appear where the ratio chamber length to wavelength is $a/\lambda = 0.21$. This is in good agreement with the $d = 0$ results in figure 12 for $h = 1.0$ m, where where $E'_{\max} = E_{\max}$ at $f = 0.82$ Hz and $a/\lambda = 0.22$. As already discussed by Falcão & Sarmento, their criteria for optimum efficiency are, in turn, consistent with those obtained by Lighthill (1979) for resonant ducts.

The more complicated case $b < c$ and $d \neq 0$ will not be considered in detail in this paper. However, we have no problem deriving linear equations covering this case as well. A numerical solution is still possible and not unreasonably time-consuming, in

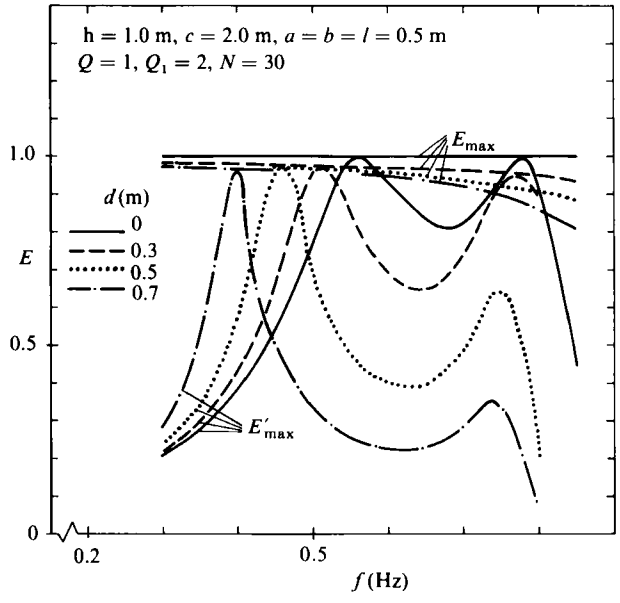

FIGURE 13. Optimum efficiencies for various barrier depths.

spite of the couplings between vertical and transverse modes. As an example of such a calculation, figure 13 shows the optimum efficiencies $E_{\max}$ and $E'_{\max}$ for an absorber in a reflecting wall when the chamber length is the same as in figure 12, and when the geometry otherwise is the same as for the $a = b = l$ case in figure 7.

Generally speaking, an increase in barrier depth makes the $E'_{\max}$ curve narrower and pushes its peak towards lower frequencies. Like the other geometrical parameters in the system the barrier depth thus has an appreciable effect on the absorbed power from a given spectral distribution of incident waves. The expected wave heights will also influence the choice of barrier depth, since the barrier should remain submerged during the operation of the power station.

8. Concluding remarks

This work on oscillating water columns in a channel was done for the purpose of providing a theoretical foundation for the construction of wave-power stations consisting of many such units in a row. We shall later return to the question of wave-power absorption by single water columns or by a few columns in a row. Also, we intend to report on an extensive experimental programme in this field. Suffice it at this point to say that there seem to be no major disagreements between theory and experiment.

A major part of this work was performed as a research project at the Norwegian Hydrotechnical Laboratory under a contract with Kværner Brug A/S, made possible through financial support from the Department of Petroleum and Energy. It is our privilege and pleasure to acknowledge the help and encouragement that we have received from our NHL project manager, Mr K. Bønke. We are also grateful for beneficial discussions with Dr B. M. Count of the Marchwood Engineering Lab-

oratories, Southampton, Dr D. V. Evans of the University of Bristol, Dr J. N. Newman of the Massachusetts Institute of Technology, Dr E. Mehlum of the Central Institute for Industrial Research, Oslo, and Drs K. Budal and J. Falnes of the Norwegian Institute of Technology.

Appendix A. Air compressibility

In calm sea the air in the chamber occupies a volume $V_C = abH$ (figure 1) and its pressure p equals the atmospheric pressure p_a. Under operating conditions the volume flux of air through a turbine fulfilling the linearity condition is

$$\frac{dV_t}{dt} = C_t p_e, \tag{A 1}$$

where C_t is the turbine constant and $p_e = p - p_a$ is the excess chamber pressure. The volume V_t is here counted as positive for air flowing from the chamber to the exterior, and negative for air flowing in the opposite direction.

As elsewhere in the paper we employ the complex notation where the actual physical quantities are the real parts of the corresponding symbolic ones. For $p_e = p_C \exp(i\omega t)$, $V_t = V_0 \exp(i\omega t)$, with $p_C = |p_C| \exp(i\phi_p)$, $V_0 = |V_0| \exp(i\phi_V)$ the actual excess pressure and turbine air volume are thus $p_e' = |p_C| \cos(\omega t + \phi_p)$ and $V_t' = |V_0| \cos(\omega t + \phi_V)$. We allow for a possible phase lag between the excess pressure and the volume flux of air by using a complex turbine constant $C_t = |C_t| \exp(i\phi_C)$. In the periodic case we thus have $|V_0| = \omega^{-1} |C_t| |p_C|$ and $\phi_V = \phi_C + \phi_p - \frac{1}{2}\pi$.

Let us assume that the actual pressure $p' = \mathrm{Re}(p)$ and volume $V' = \mathrm{Re}(V)$ of the air in the chamber are related through the ideal-gas equation $p' V'^{\kappa} = \text{constant}$, where $\kappa = 1.4$ or 1 for adiabatic or isothermal situations, respectively. A change dV' in the volume is then accompanied by a change $dp' = -\kappa(p'/V')\,dV'$ in the pressure. In the spirit of linear wave theory, i.e. on the assumption of small changes in volume and pressure, we replace the ratio p'/V' by p_a/V_C. Since the resulting relation between volume and pressure is linear, it can be used for the symbolic quantities as well, so that

$$dp = -\kappa \frac{p_a}{V_C} dV. \tag{A 2}$$

During an infinitesimal time interval dt the volume V changes by an amount

$$dV_t = C_t p_e \, dt$$

owing to the flow through the turbine and by an amount

$$dV_\eta = -A_C \, d\langle \hat{\eta}_C \rangle$$

owing to the change in chamber volume caused by the water waves. Here $\langle \hat{\eta}_C \rangle$ is the time-dependent wave elevation averaged over the chamber surface area $A_C = ab$. With $dV = dV_t + dV_\eta$, we use (A 2) to obtain

$$A_C \frac{d\langle \hat{\eta}_C \rangle}{dt} = C_t p_e + V_C (\kappa p_a)^{-1} \frac{dp}{dt}. \tag{A 3}$$

In the periodic case $p_e = p_C \exp(i\omega t)$ this becomes

$$\left.\begin{aligned} A_C \frac{d\langle\hat{\eta}_C\rangle}{dt} &= \Lambda p_e, \\ \Lambda = C_t + i\omega\Delta, \quad \Delta &= \frac{V_C}{\kappa p_a}. \end{aligned}\right\} \tag{A 4}$$

For incompressible air, on the other hand, we would have

$$dV_t + dV_\eta = C_t p_e\, dt - A_C\, d\langle\hat{\eta}_C\rangle = 0,$$

or

$$A_C \frac{d\langle\hat{\eta}_C\rangle}{dt} = C_t p_e. \tag{A 5}$$

In the present approximation, therefore, the air compressibility has the effect of replacing the actual, and possibly already complex, C_t by an effective turbine constant $\Lambda = C_t + i\omega\Delta$. For the constant κ entering the expression (A 4) for the correction term Δ, it seems appropriate to use the adiabatic value 1.4.

Appendix B. Separation of the z-dependence and definition of certain integrals over z

For harmonic waves described by the velocity potential

$$\hat{\phi}(x, y, z, t) = \phi(x, y, z) \exp(i\omega t)$$

the Laplace equation $\nabla^2\phi = 0$ can be separated by writing $\phi(x, y, z) = \tilde{\phi}(x, y)\, e_n(z)$, where

$$\left.\begin{aligned} \left[\frac{\partial^2}{\partial x^2} + \frac{\partial^2}{\partial y^2} - m_n^2\right]\tilde{\phi}_n(x, y) &= 0, \\ \left[\frac{\partial^2}{\partial z^2} + m_n^2\right] e_n(z) &= 0. \end{aligned}\right\} \tag{B 1}$$

The eigenfunctions $e_n(z)$ and eigenvalues m_n follow from the boundary conditions

$$\left.\begin{aligned} \frac{de_n(z)}{dz} &= \nu e_n(z) \quad (z = 0), \\ \frac{de_n(z)}{dz} &= (z = -h), \\ \nu &= \omega^2/g, \end{aligned}\right\} \tag{B 2}$$

where the z-axis points upwards from an origin at the surface.

Using the normalization $e_n(0) = 1$, we have

$$\left.\begin{aligned} e_n(z) &= \frac{\cos m_n(z + h)}{\cos m_n h}, \\ m_n \tan m_n h &= -\nu, \quad n = 0, 1, 2, \ldots. \end{aligned}\right\} \tag{B 3}$$

Here m_n is real for $n > 0$, while $m_0 = \mathrm{i}k$, where k is the wavenumber. For $n = 0$ the expressions (B 3) can then also be written

$$\left.\begin{aligned} e_0(z) &= \frac{\cosh k(z+h)}{\cosh kh}, \\ k \tanh kh &= \nu. \end{aligned}\right\} \tag{B 4}$$

With the present definition, the normalization integral for the eigenfunctions is

$$\left.\begin{aligned} \int_{-h}^{0} e_n(z)\, e_{n'}(z)\, \mathrm{d}z &= d_n \delta_{nn'}, \\ d_n &= \tfrac{1}{2}h\left\{1+\left(\frac{\nu}{m_n}\right)^2 [1-(\nu h)^{-1}]\right\}, \end{aligned}\right\} \tag{B 5}$$

and the other integrals over z that appear in the text are

$$\left.\begin{aligned} e_{nn'}(d) &= d_n^{-1} \int_{-h}^{-d} e_n(z)\, e_{n'}(z)\, \mathrm{d}z \\ &= [2d_n \cos(m_{n'} h) \cos(m_n h)]^{-1} \\ &\quad \times \{(m_{n'}+m_n)^{-1} \sin[(m_{n'}+m_n)(h-d)] \\ &\quad + (m_{n'}-m_n)^{-1} \sin[(m_{n'}-m_n)(h-d)]\} \end{aligned}\right\} \tag{B 6}$$

and

$$\left.\begin{aligned} g_n(d) &= -d_n^{-1} \int_{-h}^{-d} e_n(z)\, \mathrm{d}z \\ &= -2\left\{1+\frac{2m_n h}{\sin 2m_n h}\right\}^{-1} e_n^{(1)}(-d), \\ e_n^{(1)}(z) &= \frac{\sin m_n(z+h)}{\sin m_n h}. \end{aligned}\right\} \tag{B 7}$$

In the last line of (B 6) the expression $(m_{n'}-m_n)^{-1} \sin[(m_{n'}-m_n)(h-d)]$ should be replaced by $h-d$ when $n' = n$.

REFERENCES

Ambli, N., Bønke, K., Malmo, O. & Reitan, A. 1982 The Kværner mulitresonant OWC. In *Proc. 2nd Intl Symp. on Wave Energy Utilization, Trondheim*, pp. 275–295.

Count, B. M. & Evans, D. V. 1984 The influence of projecting side walls on the hydrodynamic performance of wave-energy devices. *J. Fluid Mech.* **145**, 361–376.

Evans, D. V. 1978 The oscillating water column wave-energy device. *J. Inst. Maths Applics* **22**, 423–433.

Evans, D. V. 1982*a* Wave-power absorption by systems of oscillating surface pressure distributions. *J. Fluid Mech.* **114**, 481–499.

Evans, D. V. 1982*b* Wave-power absorption within a resonant harbour. In *Proc. 2nd Intl Symp. on Wave Energy Utilization, Trondheim*, pp. 371–379.

Falcão, A. F. de O. & Sarmento, A. J. N. A. 1980 Wave generation by a periodic surface pressure and its application in wave-energy extraction. In *Proc. 15th Intl Congr. Theoretical and Applied Mechanics, Toronto.*

Lighthill, J. 1979 Two-dimensional analyses related to wave-energy extraction by submerged resonant ducts. *J. Fluid Mech.* **91**, 253–317.

SIMON, M. J. 1981 Wave-energy extraction by a submerged cylindrical resonant duct. *J. Fluid Mech.* **104**, 159–187.

SROKOSZ, M. A. 1980 Some relations for bodies in a canal, with an application to wave-power absorption. *J. Fluid Mech.* **99**, 145–162.

THOMAS, J. R. 1981 The absorption of wave energy by a three-dimensional submerged duct. *J. Fluid Mech.* **104**, 189–215.